

Low-K granophyres of the Stillwater Complex, Montana

GERALD K. CZAMANSKE

U.S. Geological Survey, Menlo Park, California 94025, U.S.A.

MICHAEL L. ZIENTEK

U.S. Geological Survey, Spokane, Washington 99201, U.S.A.

CRAIG E. MANNING

Department of Earth and Space Sciences, UCLA, Los Angeles, California 90024, U.S.A.

ABSTRACT

Small bodies of granophyre occur as a volumetrically insignificant but ubiquitous component of the Banded series of the Stillwater Complex. White to pink granophyre typically occurs as veins, 1–12 cm thick and as much as 100 m long. A geochemically similar body of coalescing alaskite dikes, associated with an occurrence of Pt-group elements in the Banded series of the complex, crops out approximately 2 km south-southeast of Picket Pin Mountain over an area 130 by 210 m.

Analyzed samples contain 77–79 wt% SiO₂ and, with one exception, less than 0.12 wt% K₂O. Albite or oligoclase and quartz, commonly in granophyric, plumose, or graphic intergrowths, commonly make up more than 97 vol% of the veins. Rare-earth-element contents of whole-rock samples and feldspar separates are as much as 100 times those of chondrites; typically, there is a pronounced negative Eu anomaly. Considering host rocks and chemistry, these rocks are comparable to the most siliceous examples of oceanic plagiogranite. The Stillwater granophyres, however, are enriched in Si, Th, U, and LREEs, and depleted in K, Fe, and Eu, relative to oceanic granophyres.

The relatively voluminous granophyres of classic diabase-granophyre associations contain 1.9–5.0 wt% K₂O and 57–74 wt% SiO₂; they are readily interpreted as crystallization differentiates. In contrast, we interpret granophyres of the type found in the Stillwater Complex, characterized by very low K₂O content, near-constant high SiO₂ content, and varying, commonly anomalously high CaO content, to have evolved during the latest stages of consolidation, in equilibrium with a high-temperature aqueous chloride solution. We suggest that these granophyres may typically represent material transported by and precipitated from these solutions.

INTRODUCTION

Silicic differentiates associated with mafic intrusions have been of interest to petrologists since the turn of the 20th century. In his historic treatise on the evolution of igneous rocks, Bowen (1915) stated that the diabase-granophyre “. . . association is of fundamental importance in petrogenetic theory and will be made the starting point for discussion of the geologic evidence supporting crystallization differentiation.” Grout (1918) followed shortly after with his classic paper on the mafic and red rocks of the Duluth Complex, Minnesota. Such granophyres as those analyzed by Grout and, for example, by Hamilton (1959) from the Wichita lopolith, Oklahoma, by Ernst (1960) from the Endion Sill, Duluth Complex, and by McDougall (1962) from Red Hill, Tasmania, are relatively voluminous and contain 57–74 wt% SiO₂ and 1.9–5.0 wt% K₂O. Thus, classic silicic differentiates vary in composition and have K₂O contents commensurate with concentration in residual melts.

Falconer (1906) was apparently the first to mention and analyze the class of low-K granophyres that appear to predominate in the Stillwater Complex. We are aware of more lengthy, lucid discussions of comparable rocks by Shannon (1924), von Eckermann (1938), and Walker (1940). Distinguishing features of these granophyres are (1) occurrence as thin (3–10 cm) discontinuous veins or semiellipsoidal blobs as much as 1 m across, (2) granophyric to graphic intergrowths of albite or oligoclase and quartz (Barker, 1970), (3) K₂O contents well below 1 wt% and Na₂O contents of 5.7–7.2 wt%, and (4) varying, commonly high CaO contents ranging from 0.70 to 3.76 wt%. After studying relations in intrusive diabase at Goose Creek, Virginia, Shannon (1924, p. 29) concluded that “. . . the aplites are . . . final products of a process of magmatic differentiation which yielded small amounts of a fluid acid residuum rich in water.” He noted that at 71.6 wt% SiO₂ (0.70 wt% K₂O), the aplites are more SiO₂ rich “. . . than any differentiate of the Triassic diabase yet described.” Von Eckermann (1938) published analyses from

eight localities of what he termed "sodic rest-magmas" and reasoned that they could "... be used to gain additional knowledge of the laws governing the closing stages of magmatic activity." The first two of these analyses, representing "albitophyre," were rocks that cut diabase on the east coast of Sweden. They have SiO_2 contents (75.95 and 78.12 wt%), K_2O contents (0.27 wt% and trace amounts), and textures more similar to those of Stillwater granophyres than any other exposed rocks of which we are aware. Von Eckermann's other examples contain less SiO_2 and more K_2O . Although he could offer no explanation for the contrast, von Eckermann noted that the differentiates occurring in diabase are characterized by negligible K_2O content and granophyric textures, whereas those occurring in gabbro contain comparable amounts of K_2O and Na_2O . Sinton and Byerly (1980) stressed that in Deep Sea Drilling Project (DSDP) Hole 417D in the western Atlantic Ocean, low-K granophyres occur in massive basaltic units greater than 10 m thick.

Finally, Walker (1940) noted that both the upper and lower chilled phases of the Palisades Sill are traversed at numerous localities by white veins, as much as 8 cm across. These veins, which are comparable in composition to those discussed by Falconer (1906), Shannon (1924), and von Eckermann (1938), were interpreted by Walker to represent a final magmatic residuum and to verge on the hydrothermal stage. Walker emphasized that, in contrast, pegmatitic schlieren in diabase typically have compositions quite similar to that of normal diabase and must represent segregation of liquid at an earlier stage.

FIELD AND MICROSCOPIC CHARACTERISTICS

Volumetrically insignificant amounts of white to pink veins composed nearly exclusively of quartz and sodic plagioclase (Ab_{77-94}) commonly occur in two- and three-phase mafic cumulates of the Banded series of the Stillwater Complex (Figs. 1A and 1B). Although these veins can be found in cumulates as low as the Norite I zone (for terminology, see Zientek et al., 1985), they are notably more abundant in the Gabbronorite III zone, the uppermost unit of the complex. We have not observed them within the major plagioclase cumulates (anorthosites), possibly because of the absence of color contrast, although we have traversed these units extensively. The irregular veins are typically oriented at high angles to cumulate layering, but rare examples of veins subparallel to layering have also been noted; they may be as much as 12 cm thick and 100 m long. Stan Todd (personal communication, 1989), who has spent many months mapping Banded-series cumulates, also observed these siliceous rocks to occur as transgressive inverted "tear drops" about 1 m high and 0.3 m across. The veins were emplaced after consolidation of the cumulates, as evidenced by sharp linear contacts, by narrow tapering granophyric veinlets that isolate thin wedges of oriented cumulate against wider veins, and by centimeter-size flakes of adjacent cumulate within veins. Some veins, represented by the analyses listed in Table 1, contain only

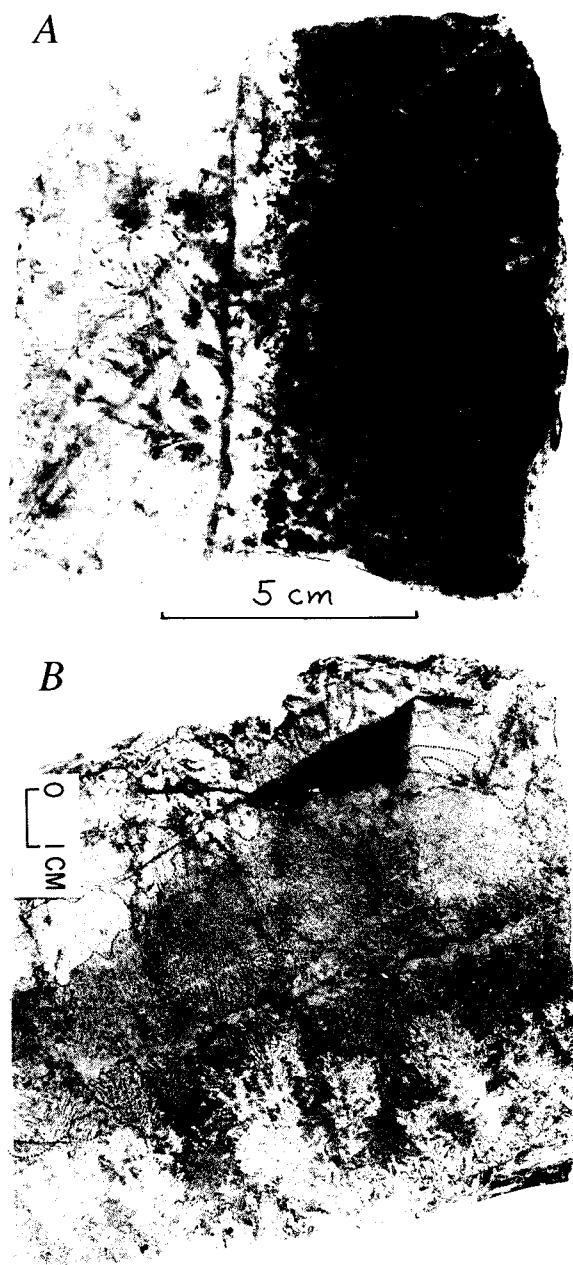


Fig. 1. (A) Oligoclase-quartz granophyre (sample 84CML16) cutting plagioclase-olivine-augite cumulates of Olivine-bearing zone II. Full width of vein is shown. Epidote veinlet runs parallel to right contact, 1 cm within granophyre. (B) Potassic granophyre (sample 85PPC8), stained with amaranth and sodium cobaltinitrite. Branching plumose albite-quartz granophyric blades grew inward from plagioclase-augite-bronzite cumulates of Gabbronorite zone III. Center of vein contains a discontinuous stringer of quartz (inconspicuous in photograph), 2–5 mm wide, and an asymmetric, irregular zone of granophyre in which the feldspar component is perthite (Table 3). Perthitic medial part of vein is enhanced by dotted contact. Specimen is full vein width.

TABLE 1. X-ray fluorescence analyses and norms for whole rocks and feldspar-quartz separates

	Veins						Alaskite	
	84CML16	84PPC8	85PPC2	87MVZ2	87PPZ29	87TAZ5	86PPZ5	S69-19
SiO ₂	77.9	77.9	77.3	79.7	78.1	77.5	78.0	77.1
Al ₂ O ₃	12.3	11.8	12.6	11.6	12.3	13.4	12.5	13.0
Fe ₂ O ₃	0.31	0.25	0.35	0.24*	0.62*	0.29*	0.14	0.00
FeO	0.12	0.24	0.32	—	—	—	0.28	0.39
MgO	0.25	0.33	0.32	0.58	0.46	0.17	0.42	0.00
CaO	3.54	0.65	0.90	2.39	0.82	0.48	2.96	2.13
Na ₂ O	4.18	4.79	6.26	3.87	6.40	7.24	4.29	5.65
K ₂ O	0.05	2.26	0.06	0.13	0.02	<0.02	<0.02	0.12
TiO ₂	0.03	0.08	0.07	<0.02	0.04	0.05	0.12	0.03
P ₂ O ₅	<0.05	<0.05	<0.05	<0.05	<0.05	<0.05	<0.05	0.08
MnO	<0.02	<0.02	<0.02	<0.02	<0.02	0.03	<0.02	0.006
H ₂ O ⁺	0.45	0.40	0.45	—	—	—	0.58	—
CO ₂	0.10	0.09	0.08	—	—	—	<0.01	—
LOI**	0.59	0.66	0.80	0.85	0.44	0.24	1.00	—
Total	99.34	99.03	99.05	99.45	99.27	99.47	99.80	98.51
Q	46.00	39.51	38.11	50.71	38.35	34.10	46.24	40.00
C	—	0.58	1.20	—	0.26	—	0.12	—
Or	0.29	13.35	0.35	0.77	0.12	—	—	0.72
Ab	35.28	40.54	52.83	32.75	54.16	61.26	36.39	48.70
An	14.62	3.23	4.45	11.86	4.07	2.38	14.72	9.94
Di	1.54	—	—	—	—	—	—	0.23
Hy	—	0.58	0.59	1.44	1.15	0.42	0.69	0.18
Wo	0.49	—	—	—	—	—	—	—
Mt	0.30	0.36	0.51	—	—	—	—	—
Il	0.06	0.15	0.13	—	—	0.06	—	0.06
Hm	0.10	—	—	0.24	0.62	0.29	0.47	—
Ru	—	—	—	—	0.04	0.02	0.12	—
Ap	—	—	—	—	—	—	—	0.18
Ab/(Ab + An)	0.71	0.93	0.92	0.73	0.93	0.96	0.71	0.83

Note: Analyst: Joseph Taggart, U.S. Geological Survey.

* Total Fe as Fe₂O₃.

** LOI at 900 °C. H₂O and CO₂ values not included in total.

traces of an altered mafic mineral; others contain conspicuous patches (maximum 2 cm across) of intergrown, coarse-grained tremolitic to actinolitic amphibole (e.g., Carlson and Zientek, 1985, their Fig. 11) that may constitute 10–15 vol% of the vein; in rare pegmatitic segregations, hollow amphibole crystals approach 30 cm in length. There is no indication in the field or in thin sections that vein selvages have been quenched against cumulates. In several occurrences, macroscopic features (see Fig. 1B and sample descriptions) suggest that the veins grew more or less symmetrically inward from cumulate walls. Where these features are observed, a transition occurs from graphic or granophyric to pegmatitic textures and, in sample 84PPC8, from albitic plagioclase to K-bearing perthitic feldspar.

About 40 thin sections of silicic veins have been examined, and we analyzed six vein samples that are reasonably fresh and can be regarded as representative. Analyzed samples of the veins represent full vein widths from which the cumulate wallrocks have been removed; we avoided amphibole-rich and coarsely pegmatitic veins. In thin section, most veins display incipient to spectacular granophyric to graphic textures (Figs. 2A and 2B). The alaskite at Picket Pin Mountain approaches a medium-grained equigranular texture, and sample 87TAZ5 has an aplitic texture. This variation in texture is not

reflected in major-element composition (Table 1). The silicic veins are varyingly altered, and a single well-defined veinlet of epidote commonly records passage of late solutions. Relative degree of alteration is reflected in the data listed in Table 1; for example, the ratio 100 Ab/(Ab + An) calculated for sample 84CML16 for the whole rock (total vein) is 71, whereas that for the feldspar-quartz separate is 83. Microscopic and electron-microprobe studies show widespread development of micrometer-size grains of epidote in this sample, and a vein of epidote (Fig. 1A) 1.5–2 mm wide was analyzed with the whole-rock sample. The feldspar-quartz concentrates analyzed in this study were obtained from a wet-sieved 100 to 200-mesh sample split that was passed first through a Carpco splitter. Using of heavy liquids (specific gravities, 2.67 and 2.77) produced a concentrate that was passed through a Frantz isodynamic separator at maximum-current and low-angle settings.

As indicated by the analyses listed in Tables 1 and 2, granophyric intergrowths are typically between plagioclase and quartz (note that we deviate from Barker, 1970, by not restricting the term “granophyre” to alkali feldspar-quartz intergrowths). Barker (1970) and Černý (1971) noted that graphic intergrowths between plagioclase and quartz are not uncommon but simply less studied than those between microcline microperthite and quartz. In

TABLE 1—Continued

	Mouat quartz monzonite			Feldspar-quartz separates			
	NB17-341	84CML16	84PPC8	85PPC2	86PPZ5	S69-19	NB17-341
SiO ₂	71.5	85.2	80.8	80.7	82.3	79.7	81.5
Al ₂ O ₃	14.4	9.11	11.2	11.8	10.5	12.6	11.2
Fe ₂ O ₃	2.40*	0.06*	0.16*	0.24*	<0.04*	<0.04*	0.21*
FeO	—	—	—	—	—	—	—
MgO	0.78	0.14	0.17	0.16	0.10	<0.10	0.13
CaO	2.43	1.33	0.46	0.80	2.03	1.46	2.45
Na ₂ O	3.63	3.92	4.55	5.90	3.97	5.43	3.79
K ₂ O	3.71	0.03	2.31	0.04	<0.02	0.11	0.49
TiO ₂	0.17	<0.02	<0.02	<0.02	<0.02	<0.02	<0.02
P ₂ O ₅	0.03	0.01	<0.002	0.006	0.05	0.005	0.005
MnO	0.03	<0.02	<0.02	<0.02	<0.02	<0.02	<0.02
H ₂ O ⁺	—	—	—	—	—	—	—
CO ₂	—	—	—	—	—	—	—
LOI**	0.75	0.65	0.72	0.73	0.40	0.70	0.40
Total	99.83	100.49	100.41	100.41	99.45	100.18	100.21
Q	30.17	59.20	44.18	44.10	54.71	44.20	52.23
C	0.28	0.42	0.75	1.19	0.28	1.77	—
Or	22.03	0.18	13.61	0.24	—	0.64	2.90
Ab	30.87	33.12	38.39	49.67	33.59	45.51	32.08
An	11.72	6.59	2.28	3.95	10.07	7.18	12.11
Di	—	—	—	—	—	—	0.05
Hy	1.28	0.23	0.28	0.26	0.25	—	0.20
Wo	—	—	—	—	—	—	—
Mt	—	—	—	—	—	—	—
Il	0.06	—	—	—	—	—	—
Hm	2.42	0.06	0.16	0.24	—	—	0.21
Ru	0.14	—	—	—	—	—	—
Ap	0.13	—	—	—	—	—	—
Ab/(Ab + An)	0.73	0.83	0.94	0.93	0.77	0.86	0.73

the vein represented by sample 84PPC8, flames of albite-quartz granophyre grew inward from cumulate walls (Figs. 1B and 2B). As seen in Figure 1B and substantiated by the electron-microprobe data of Table 3, perthite later became the stable feldspar component of the granophyre and is now intergrown with quartz at the center of the vein. Coarse-grained feldspar-quartz pegmatite in the core of sample 87PPZ1 was initially assumed also to contain alkali feldspar, but the feldspar was shown by Gunier-Hägg X-ray diffraction study to be well-ordered, nearly end-member albite (An₀₋₁). On the basis of 67 indexed diffraction maxima read over the 2θ range 12–65°, Robert F. Martin (written communication, 1990) determined: *a* = 8.1342 Å ± 0.0011, *b* = 12.7921 Å ± 0.0039, *c* = 7.1586 Å ± 0.0007, α = 94.267° ± 0.012, β = 116.609° ± 0.009, γ = 87.706° ± 0.009, and *V* = 663.70 ± 0.33 Å³. Aside from the fresh amphibole occurring as clots in some veins and a few preserved needlelike grains of biotite in some thin sections of sample 84PPC8, trace contents of mafic minerals in the veins have been altered to chlorite, ranging in color from pale green to tan.

Contacts between veins and cumulates are curvilinear to irregular at the microscopic scale, commonly smooth and featureless; cumulus, wallrock plagioclase grains are commonly broken (Figs. 1A and 2B). In most samples, pyroxene next to veins in host cumulates shows alteration to amphibole and chlorite, but wallrock plagioclase is typically unaltered. Across a rare reaction rim 0.3 mm

wide, in which twinning is continuous, the An content of a broken cumulus plagioclase grain drops from 63 to 30 mol% against granophyre. In some samples, blebby, complex reaction zones between quartz and secondary amphibole have formed where the silicic veins are in contact with pyroxene.

Small grains of titanite (maximum 0.3 mm long) occur in sample 86PPZ5 from the alaskite near Picket Pin Mountain, and altered remnants presumed to have been titanite have been noted in several other samples. Sparse equant brown zircons, typically <100 μm across but as much as 250 μm across in sample S69-19, are zoned and contain inclusions. Rare, anhedral, zoned allanite grains, as large as 6 by 14 mm, are present in sample 87PPZ6 from the alaskite contact. Cursory SEM study revealed a uranothorite grain, 30 by 100 μm, next to a zircon in sample S69-19 and a thorite grain, 20 by 40 μm, in sample 85PPC2.

THE ALASKITE AT PICKET PIN MOUNTAIN

The large mass of alaskite that crops out over an area of approximately 130 by 210 m about 2 km south-southeast of Picket Pin Mountain (Fig. 3) has been studied for some time. The analyses listed in Tables 1 and 2 give it no notable distinction in composition from the granophyric veins, and textures within it can be subgranophyric; yet the occurrence is remarkable in terms of its size and the complexity of its contact relations. Within a

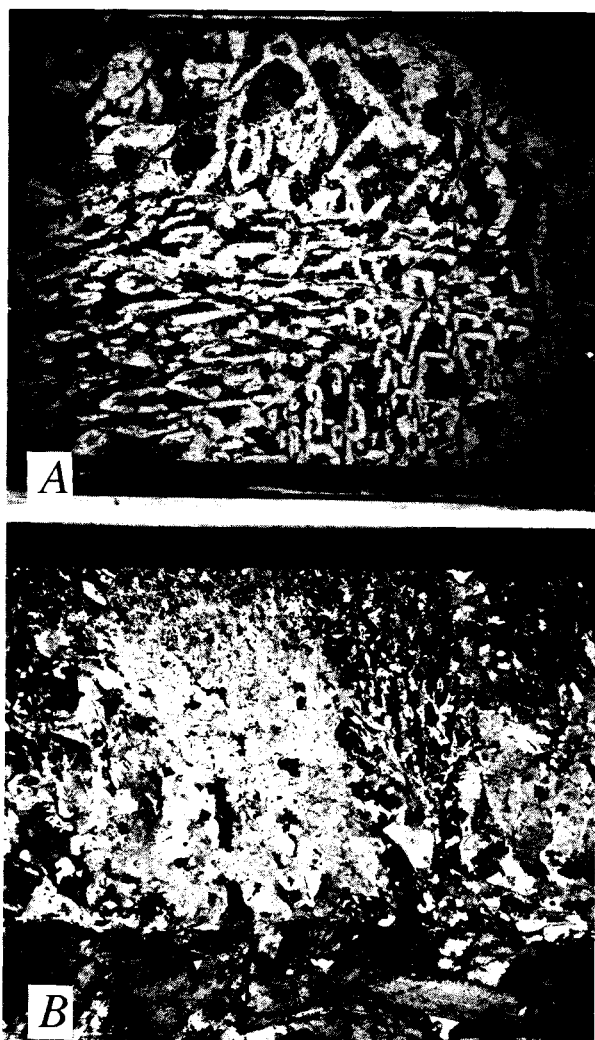


Fig. 2. (A) Photomicrograph of oligoclase-quartz granophyre, sample 84CML16. Full thin-section width of 21 mm is shown. Plane-polarized light. (B) Photomicrograph of albite-quartz granophyre that grew upon plagioclase-augite-bronzite cumulate host, sample 84PPC8. Width of photograph is 20 mm. Crossed Nicols.

structurally complicated area, Segerstrom and Carlson (1982) mapped the alaskite as cropping out within Anorthosite zone I and noted the occurrence of several smaller silicic bodies nearby in the Banded series. Drilling and mapping suggest a complex geometry, characterized by multiple alaskite dikes and quartz-rich segregations and veins, discordant to the Stillwater cumulates that dip about 60° north-northeast. Attitudes of contacts between alaskite and cumulates range from subvertical to 35° south. Mappable among rubble within the perimeter of the alaskite are Stillwater cumulates, with layering discordant to that of the complex as a whole, that appear to represent a large tilted block. Reconnaissance mapping of the poorly exposed mass at a scale of 1:1200 (C. A. Carl-

son, written communication, 1988) revealed at least eight localities where conspicuous concentrations (maximum 10 cm thick and several meters long) of chromite and sulfide minerals, or of sulfide minerals in quartz-rich segregations, occur along the margins of the alaskite (Fig. 3). The first (1968) Pt-group-element (PGE) occurrence considered to be of interest by Johns-Manville Corp. geologists was associated with one of these selvages (Conn, 1979); a bulk sample assayed 5.1 ppm Pt, 3.4 ppm Pd, 0.4 ppm Rh, 0.24 wt% Ni, 0.03 wt% Cu, and 5 wt% Cr₂O₃. In 1969, six inclined holes as much as 170 m long (four are shown in Fig. 3) were drilled to explore the mass at depth. These holes penetrated varying thicknesses of discordant siliceous rock, with a maximum intercept thickness of 18 m. One drill core contained 12 alaskitic or quartzose intercepts within 100 m of the collar (none > 5 m thick).

Although chromite-bearing selvages have been generally accepted as occurring at the contacts of the alaskite at Picket Pin Mountain and speculated to represent material carried up from the Ultramafic series, the chromite of these selvages has not been studied. The only analyses known to us are of relatively sulfide-rich selvage samples taken for measurement of PGE contents; most samples analyzed by the Johns-Manville Corp. were comparable to that reported by Conn (1979) and contained only 1–2 wt% Cr (Bob Mann, personal communication, 1989). We have now confirmed that parts of some selvages contain as much as 60 vol% chromite (Fig. 4), none of which has a composition comparable to that of Ultramafic-series chromite, which contains 4–10 wt% MgO and 13–27 wt% Al₂O₃.

The bulk of the chromite in sample 87PPZ6 consists of a mixed population of rounded to subhedral grains, ranging in size from 50 to 200 μm across. These grains do not polish well; larger grains are mildly pitted and cracked in their centers and heavily dissected by tiny radial channelways at their margins, and it is difficult to find coherent areas more than a few micrometers across in smaller grains. Most of these grains fall in the compositional range shown under the heading "Cores" in Table 4, but intermingled, texturally indistinguishable grains have a distinct, notably more Al-rich composition (Table 4, first two columns). The heavily dissected rims may or may not be characterized by Fe depletion and Cr enrichment. In scattered clusters of grains (Fig. 4), rounded cores of texturally and chemically typical chromite are surrounded by bright rims (maximum 20 μm thick) of notably more Cr-rich composition. Their sharply bounded, ringlike form and the occurrence of chromite identical in composition as a population of bright euhedral to subhedral grains, 20 to 50 μm across, appear to distinguish this material from that studied as ferritichromit from the Ultramafic series of the Stillwater Complex by Beeson and Jackson (1969), which is described as a volume-for-volume replacement product. Finally, within a standard polished thin section, 15–20 better polished, large subhedral phenocrysts (maximum 300 μm across) seem to

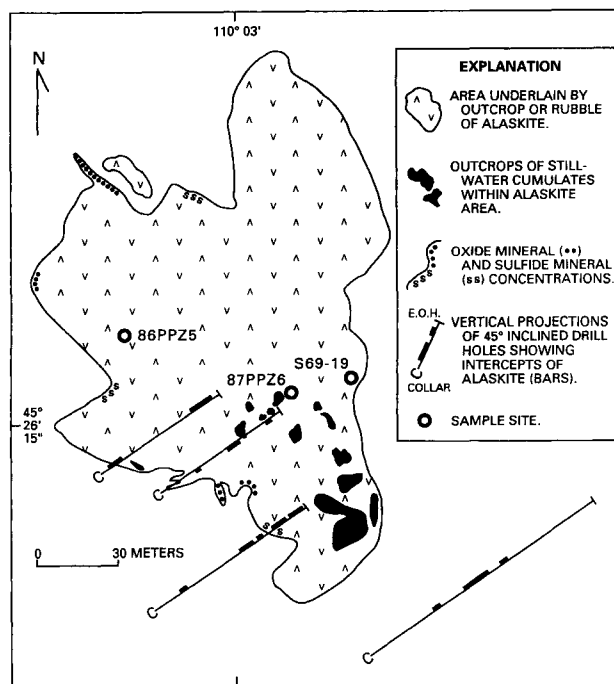


Fig. 3. Reconnaissance sketch map of the alaskite occurrence at Picket Pin Mountain. Diamond drilling by the Johns-Manville Corporation.

represent yet another population of grains. Occasional rimming of these larger grains by bright chromite suggests that their growth was more or less contemporaneous with that of the chromite we refer to as "cores," as does their only marginally distinct composition (Table 4).

In considering PGE-enrichment processes in the Stillwater Complex, Boudreau et al. (1986) and Boudreau and McCallum (1986, 1989) argued that Cl-rich fluids exsolved and circulated through the Stillwater cumulate sequence. We suggest that the Cr and chalcophile elements contained in the selvages were derived from Stillwater mafic cumulates by the action of aqueous chloride solutions and that the alaskite at Picket Pin Mountain represents a fortuitous exposure of coalesced vein material comparable in origin to that in the smaller veins. Chromite- and sulfide-rich selvages, as well as complex silicate reactions with the host cumulates, indicate that despite the competency of these cumulates, they were quite reactive during deposition of the silica-rich rocks.

GRANOPHYRE COMPOSITION

The six samples of granophyric to aplitic veins and two alaskite samples are remarkably similar in major-element composition, differing only in the proportions of Ca, Na, and K (Table 1). The rocks are as silicic as any reported in the literature in association with mafic intrusions or ophiolitic complexes. Sample 84PPC8 is anomalous in its higher K content, reflecting the presence of perthitic alkali feldspar as well as plagioclase (Fig. 1B; Table 3). Normative-quartz contents of the whole-rock samples

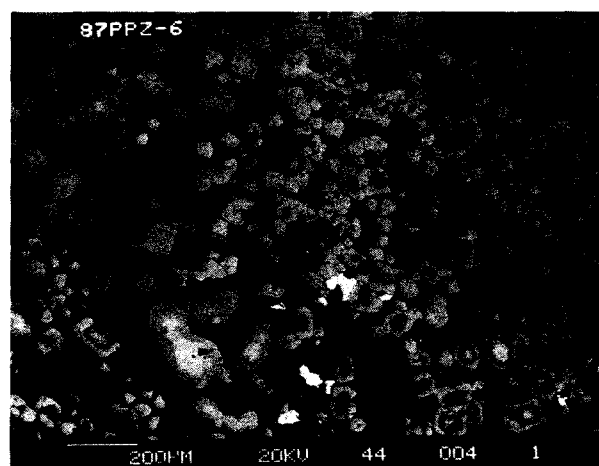


Fig. 4. Backscattered-electron image of polished section of chromite-enriched selvage to the alaskite at Picket Pin Mountain, sample 87PPZ6. Late overgrowths and bright, small euhedral crystals rich in Cr, contrast with corroded earlier grains. No large phenocrysts are shown.

range from 34.0 to 50.7%, with four of eight values in the narrow range of 38.1–40.0%. This range is identical to that reported in many studies of granophyric intergrowths involving alkali feldspar (Barker, 1970, his Table 3). Major-element analyses of the feldspar-quartz separates (Table 1) provide a good estimate of the feldspar compositions, which range from An₇ to An₂₃. Because quartz could not be adequately separated from these feldspars, we used the normative proportions of quartz and feldspar to calculate factors for determining the minor-element contents of the feldspars (see footnote to Table 2).

Electron-microprobe analyses were obtained for representative feldspars in samples 84PPC8 and 84CML16. The first two columns of Table 3 list analyses of the components of the perthitic alkali feldspar that is interpreted to have replaced or grown upon early-formed albite-quartz granophyre in sample 84PPC8; the compositions are of nearly pure albite and orthoclase. The albitic component of the perthite has a composition virtually identical to that determined for the albitic component of coarse-grained granophyre in two thin sections of the vein (Table 3; Fig. 2B). Analysis of the plagioclase component of the granophyre in sample 84CML16 (Fig. 2A) was not straightforward, presumably owing to incipient development of fine-grained epidote during plagioclase alteration. Because the effect of this alteration is to reduce Ca content, the most sodic points analyzed are interpreted to represent altered plagioclase (Table 3, last column). Conversely, the more calcic plagioclase is interpreted to represent the original plagioclase component in the granophyre (Table 3, second-to-last column). The 100 Ab/(Ab + An) ratio of 80, calculated from microprobe data for the Ca-rich areas, agrees reasonably well with the value of 83 obtained from analysis of the feldspar-quartz separate (Table 1). Note that plagioclase in four of the

TABLE 2. Minor- and trace-element data for whole rocks and feldspar separates (in ppm, except for K and Ti in wt%)

	Whole rocks						
	84CML16	84PPC8	85PPC2	86PPZ5	S69-19	NB17-341	81CMC17
Ba	31	30	28	71	74	870	23
Co	—	—	—	3.05	0.15	4.67	20
Cr	1.9	<2	<3	3.3	1.9	10.8	224
Cs	0.21	1.70	0.22	<0.05	0.31	0.59	<0.3
Hf	1.64	3.21	4.17	3.85	3.39	2.48	<0.4
K	0.04	1.92	0.07	0.02	—	3.09	0.05
Li	<3	5	7	<3	—	11	<3
Mn	105	125	120	65	—	300	480
Mo	<2	<3	<11	—	—	<2	—
Nb	<10	20	18	15	<10	<10	—
Ni	12	<10	17	70	5.2	17	180
P	—	—	—	—	—	0.013	0.002
Rb	5.6	170	<10	1.2	2.4	80	<10
Sc	2.03	2.84	2.81	2.95	0.13	3.03	20.2
Sr	120	14	16	150	150	215	120
Ta	—	—	—	2.06	0.07	0.29	<0.1
Th	14.7	19.7	51.8	40.5	31.5	19.7	<0.2
Ti	0.034	0.062	0.056	0.105	—	0.130	0.062
U	4.6	18.9	39.2	14.0	10.9	2.19	<0.02
Y	13	26	41	16	<10	9	3
Zn	8	7	7	9	5	57	21
Zr	40	70	120	100	90	90	<100
La	8.5	14.6	27.5	37.8	3.53	38.7	0.7
Ce	18.8	29.5	56.2	71.6	4.0	65	1.5
Nd	8.3	8.4	18.9	23.9	—	18.3	<5
Sm	1.58	2.01	3.99	4.17	0.69	3.10	0.25
Eu	0.09	0.08	0.15	0.39	0.04	0.83	0.20
Tb	0.43	0.61	1.34	0.39	0.21	0.50	0.09
Dy	—	—	—	2.27	—	—	—
Yb	1.06	2.72	3.74	1.56	0.68	0.67	0.25
Lu	0.15	0.40	0.60	0.26	0.12	0.11	0.06

Note: Data for Ba, K, Li, Mn, Sr, Y, and Zn by ICP; for P by emission spectroscopy; for Nb and Zr by EDXRF, except whole-rock values for Nb by ion-exchange + ICP; remainder by INAA. Values for Ba, Ni, Rb, Sr, Y, and Zn supported by EDXRF. Analysts: ICP, Paul Lamothe; emission spectroscopy, Chris Heropoulos; EDXRF, Bi-shia King; whole-rock Nb, Terry Fries; INAA, James Budahn; all with the U.S. Geological Survey.

* Data corrected for dilution by quartz, per Table 1. Multiplication factors: 84CML16, 2.45; 84PPC8, 85PPC2, and S69-19, 1.79; 86PPZ5, 2.21; NB17-341, 2.09.

** Values in parentheses by isotope dilution. Also 81CMC17, Gd-0.056 and Er-0.014; 83BRL1, Gd-0.162 and Er-0.047.

samples analyzed (84CML16, 87MVZ2, 86PPZ5, and S69-19) has a significantly higher Ca content than would be expected for rocks containing 77–79 wt% SiO₂ that had originated by crystallization differentiation; such Ca contents are entirely appropriate in equilibrium with an aqueous chloride solution (Orville, 1972; Schliestedt and Johannes, 1990).

Minor- and trace-element data (Table 2) for the whole veins and the feldspars show substantial variation, some of which is not readily explicable. As an additional measure of comparison, we also list data in Tables 1 and 2

for (1) drill-core sample NB17-341 of the Mouat quartz monzonite, a composite body that intruded the southeast margin of the Stillwater Complex shortly after its emplacement; (2) sample 81CMC17 from the upper part of the Gabbronorite II zone (GN II); and (3) sample 83BRL1 of the Gabbronorite III zone (GN III) near the top of the exposed complex. Cumulates of GN II are the host for sample 84CML16 and those of GN III host samples 84PPC8, 85PPZ2, and 87PPZ29.

Before comparing the minor- and trace-element data listed in Table 2 with those for other rocks, several ob-

TABLE 3. Electron-microprobe analyses of feldspars in Stillwater granophyre

	84PPC8.2	84PPC8.1	84CML16
SiO ₂	64.4*	68.5*	68.4
Al ₂ O ₃	18.3	19.3	19.8
CaO	0.10	0.11	0.07
K ₂ O	15.9	0.05	0.05
Na ₂ O	0.31	11.8	11.7
SrO	0.09	0.08	0.10
FeO	0.03	0.03	0.02
MgO	0.03	0.00	0.00
Total	99.16	99.87	100.14
Ab/(Ab + An)	—	99	99

* Components of perthite.

** Low-Ca and high-Ca count rates; see text.

TABLE 2—Continued

	Feldspar separates							
	84CML16*	84PPC8*	85PPC2*	86PPZ5*	S69-19*	NB17-341*	81CMC17	83BRL1
Ba	127	72	75	141	128	376	32	120
Co	2.52	0.21	0.43	1.44	0.16	1.09	0.81	0.89
Cr	<2.2	<2	<1.4	0.88	0.98	1.07	1.0	<1.0
Cs	0.49	2.94	0.32	0.07	0.38	0.21	<0.05	0.09
Hf	3.31	1.70	2.81	0.60	0.88	0.61	<0.07	0.06
K	—	—	—	—	—	—	0.06	0.20
Li	—	—	—	—	—	—	<3	<3
Mn	—	—	—	—	—	—	25	39
Mo	—	—	<9	—	—	<4	—	—
Nb	<25	<18	18	<22	<18	<21	<10	<10
Ni	<54	<14	15	26.1	<7	<21	—	—
P	0.010	0.002	0.005	—	0.004	0.004	0.002	0.001
Rb	4.4	347	5.6	0.88	5.4	21	<4	3.4
Sc	3.16	1.22	1.63	0.51	0.05	0.42	0.15	0.21
Sr	220	<18	21	252	222	397	170	225
Ta	4.46	2.20	3.78	0.42	0.04	<0.08	<0.05	<0.08
Th	21	10.8	35.8	15.6	9.54	3.51	<0.06	0.08
Ti	—	—	—	—	—	—	0.014	0.027
U	7.08	12.2	26.9	4.35	3.40	1.32	<0.4	<0.2
Y	<25	<18	<18	<22	<18	—	<1	<1
Zn	10	5	4.5	5.3	6.4	29	9	12
Zr	44	47	79	42	32	33	14	14
La	11.6	18.1	26.0	5.35	0.63	33.4	0.92(0.930)**	1.84(1.870)
Ce	26.0	32.2	54.0	6.67	<1.8	46.2	1.27(1.516)	2.6(2.776)
Nd	14.2	9.9	18.8	2.32	<5.4	13.0	<6(0.526)	<5(1.002)
Sm	2.38	1.54	3.67	0.49	0.18	1.40	0.07(0.076)	0.18(0.194)
Eu	0.10	0.13	0.20	0.27	0.02	1.09	0.26(0.270)	0.60(0.660)
Tb	0.64	0.38	1.04	0.07	0.07	0.15	<0.03	0.022
Dy	—	—	—	—	—	—	—(0.040)	—(0.115)
Yb	1.68	1.68	2.65	0.27	0.20	0.19	<0.10(0.008)	<0.07(0.040)
Lu	0.23	0.23	0.38	0.04	0.04	0.04	<0.02	0.01

servations are in order. (1) In general, analyses of the feldspar separates are consistent with or comparable to those for the whole-rock samples, allowing for the presence of 34–50 vol% quartz in the latter. Still, minute inclusions may remain in mineral separates, and we hesitate to unequivocally ascribe all the elements reported for feldspar to that mineral. (2) Pale-pink vein material deposited as sample 85PPC2 and as the early part of sample 84PPC8 in the Picket Pin cirque is atypical (low Sr and high Nb and Y contents, high Th/U ratio). Sample 84PPC8 is uniquely enriched in K, Rb, and Cs. Association with a hydrothermally leached selvage, a Th/U ratio near 1 that may reflect hydrothermal mobilization of U, and formation of late perthitic alkali feldspar suggest that sample 84PPC8 represents an unusual additional stage in the evolution of the fluid phase. In considering analyses that showed a greater contrast in K₂O content than samples 85PPC2 and 84PPC8, Walker (1940, his Table 7) proposed that segregations richer in K represent an earlier stage of evolution. However, textures suggest that the perthitic alkali feldspar in sample 84PPC8 is a late-stage product (Fig. 1B). (3) Th/U ratios in the silicic rocks vary unusually and may approach 1. (4) Many elements are remarkably depleted in alaskite sample S69-19 in comparison with alaskite sample 86PPZ5. (5) Sc, Hf, and Ta are much less abundant in feldspar separates from the alaskite samples than in those from the transgressive veins.

On the basis of host rocks, chemical composition, and

mode of origin, the closest well-studied analogues to the Stillwater granophyres are found among oceanic plagiogranites associated with ophiolites. For these plagiogranites, the best data sets known to use are those of Thompson (1973), Coleman and Peterman (1975), Coleman and Donato (1979), and Gerlach et al. (1981). Most analyzed oceanic plagiogranites contain less SiO₂ and more Fe and K than the Stillwater silicic rocks. For example, the six oceanic plagiogranites represented by the dotted field in Figure 5A contain from 69.7 to 76.0 wt% SiO₂, 1.56 to 5.04 wt% FeO (Fe_{tot}), and 0.12 to 0.98 (average 0.38) wt% K₂O. In comparison with plagiogranites containing more than 72 wt% SiO₂, the granophyres of the Stillwater Com-

TABLE 4. Electron-microprobe analyses of chrome spinels from a selvage to the alaskite at Picket Pin Mountain (sample 87PPZ6)

	High Al		Cores (7)*		Phenocrysts		Late (4)
SiO ₂	1.04	1.12	0.00–0.27	0.00	0.00	0.33–0.53	
TiO ₂	1.48	1.17	0.69–1.48	0.55	0.59	0.30–0.80	
Al ₂ O ₃	15.3	16.5	3.60–5.68	6.30	6.37	6.45–8.59	
Cr ₂ O ₃	37.7	37.6	32.7–34.7	36.4	37.4	48.5–50.1	
V ₂ O ₅	0.43	0.43	0.20–0.23	0.25	0.28	0.32–0.41	
FeO [†]	37.6	37.6	54.7–56.8	51.5	51.2	34.8–35.9	
MnO	1.71	1.67	1.34–1.48	1.59	1.31	1.69–1.80	
MgO	0.64	0.87	0.09–0.16	0.17	0.32	0.17–0.30	
CaO	0.35	0.05	0.01–0.10	0.00	0.00	0.09–0.16	
Total	96.25	97.01		96.75	97.47		

* Number of grains included in range.

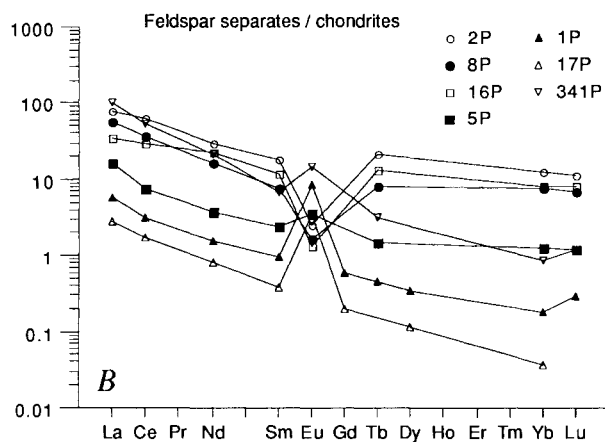
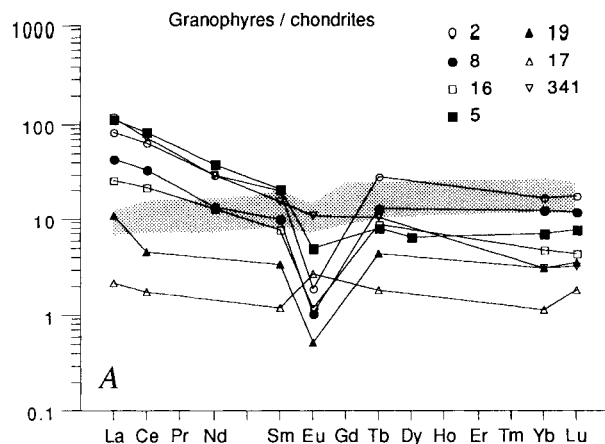


Fig. 5. Chondrite-normalized REE patterns (calculated with Spider; Wheatley and Rock, 1988). (A) Stillwater granophyric veins (2, 8, 16), the alaskite at Picket Pin Mountain (5, 19), Stillwater gabbro (17), and the Mouat quartz monzonite (341), with a shaded field for oceanic plagiogranite. (Only trailing numbers from Table 2 have been used to identify samples.) Included in the field for oceanic plagiogranite are samples from the Semail and Troodos ophiolites (OM-31, OM-32, and 100-D; Coleman and Donato, 1979) and the Canyon Mountain ophiolite (CMG55A, CMG191, OC114, and BCM-3; Gerlach et al., 1981). (B) Corrected feldspar separates. (Because of quality, data for sample 83BRL1 are plotted in lieu of those for sample S69-19. Isotope-dilution data plotted for samples 81CMC17 and 83BRL1, Table 2.)

plex have similar Ba, Co, Cr, Hf, Rb, Sc, Sr, Zn, and Zr contents, but Th and U contents are 10 to 100 times higher.

Rarely, aplites with a major-element composition comparable to that of some Stillwater silicic dikes have been recovered in dredge hauls from midoceanic ridges. The two analyses listed in Table 5 were reported by Miyashiro et al. (1970; minor-element data from Thompson, 1973) from a haul on the Mid-Atlantic Ridge (MAR) near latitude 24° north and by Engel and Fisher (1975) from a

TABLE 5. Analyses of aplite dredged from the Central Indian Ridge and Mid-Atlantic Ridge

	CIR	MAR		CIR	MAR
SiO ₂	76.37	78.39	Ga	180	55
Al ₂ O ₃	12.78	12.68	Co	<5	10
Fe ₂ O ₃	0.39	0.38	Cr	7	<5
FeO	0.46	0.41	Cu	5	9
MgO	0.87	0.54	Ga	21	24
CaO	0.84	0.55	Li	—	5
Na ₂ O	7.70	6.66	Nb	25	—
K ₂ O	0.07	0.06	Ni	29	6
TiO ₂	0.42	0.09	Pb	47	—
P ₂ O ₅	0.02	0.01	Sc	10	—
MnO	0.02	0.01	Sr	86	50
H ₂ O ⁺	0.25	0.41	V	9	35
Total	100.22	100.19	Y	180	95
			Yb	17	—
			Zr	550	150

haul on the Central Indian Ridge (CIR) near latitude 13°30' south. Both studies concluded that these aplites are the products of extreme, late-stage fractional crystallization of intrusive tholeiitic magma. Comparison of the trace-element data listed in Table 5 with those in Table 2 shows the aplite sample from the CIR to be relatively rich in Ba, Sc, Y, and Zr and that from the MAR to be enriched in Y. Engel and Fisher (1975) commented on the presence of zircon in the CIR aplite and an associated quartz monzonite containing 75 wt% SiO₂.

That the compositions of Stillwater granophyres are unusual is underscored by comparisons with the convenient summary of rhyolite compositions presented by Christiansen et al. (1983, Fig. 3). Inasmuch as K contents are extremely low in the granophyres, it is not surprising that Li (<8 ppm), Rb (<10 ppm), and Cs (<3.5 ppm) contents are also much lower than in rhyolites; Ba contents are also quite low (<75 ppm). Zn (<9 ppm) and Zr (<120 ppm) contents of the Stillwater silicic rocks are comparable to the lowest values reported for rhyolites, whereas Co, Hf, Nb, Sc, Ta, and Y are not distinctive. The atypically low Sr contents of samples 84PPC8 and 85PPC2 are comparable to those reported for rhyolites, but the remaining three values (120–150 ppm) are very high for high-silica rhyolite. However, these relatively elevated Sr contents are compatible with the CaO contents of these samples (2.1–3.5 wt%), in comparison to those that characterize rhyolites (0.2 to 1.2 wt%).

As shown in Figure 5A, REE-abundance patterns for the Stillwater silicic veins differ significantly from those for typical plagiogranites, displaying a distinctly negative, vs. slightly positive, slope and a notable negative Eu anomaly. REE-abundance patterns for oceanic plagiogranites are essentially an elevated midoceanic-ridge-basalt (MORB) pattern, interpreted by us to reflect REE extraction from relatively primitive mafic magmas. In contrast, REE-abundance patterns of the Stillwater granophyres are consistent with the LREE enrichment observed in plagioclase from Stillwater cumulates (Fig. 5B; Lambert and Simmons, 1988).

REE analyses show distinct patterns of Eu depletion in feldspar from Stillwater silicic rocks that contrast mark-

edly with the Eu enrichment typical of Stillwater cumulus plagioclase (Fig. 5B; Lambert and Simmons, 1988) and feldspar in general. This relation, evident not only for the corrected feldspar separates (Fig. 5B) but also for the whole-rock granophyre samples (Fig. 5A), reflects a complementary aspect in the granophyre-cumulate association. Relative to cumulus plagioclase (Fig. 5B, samples 81CMC17 and 83BRL1), feldspar in vein granophyre is also preferentially enriched in HREEs. Comparison of REE contents and patterns for samples 84CML16, 84PPC8, and 85PPC2, and for feldspar separated from them, indicates that the REE host is feldspar itself (or inseparable inclusions). Consideration of Table 2 and Figure 5 shows a quite different relation in the two alaskite samples, in that the feldspar separates have REE contents markedly lower than those in the whole rock. Moreover, for sample 86PPZ5, the whole-rock Eu anomaly is anomalously small, and the feldspar separate shows a positive Eu anomaly. We ascribe these anomalous features to the occurrence of discrete accessory titanite and allanite in the alaskite and suggest that their crystallization altered the REE complement available to feldspar. Feldspar from the two alaskite samples also contains a notably lesser fraction of whole-rock Th and U than does feldspar from the vein granophyres. Remarkably lower REE contents in the whole rock and plagioclase suggest that sample S69-19 represents crystallization in equilibrium with a depleted, late-stage fluid.

REE contents of the Mouat quartz monzonite and feldspar separated from it are comparable to those in the silicic veins, but the patterns are distinct and show the influence of another REE carrier, probably titanite. REE contents of Stillwater gabbro and cumulus plagioclase in gabbro are quite low. [The accuracy of the instrumental neutron-activation analyses for REEs is indicated by the isotope-dilution data for the gabbro plagioclase (An₇₅₋₈₀; Table 2).]

Electron-microprobe analyses of F-bearing tremolitic to actinolitic amphiboles contained in two unanalyzed silicic veins are listed in Table 6. The actinolitic amphibole, which is relatively unzoned, is found in sample 87PPZ3 from a silicic vein that cuts gabbroic cumulates above the mafic pegmatite at locality 13 of Carlson and Zientek (1985, p. 269). The slightly zoned tremolitic amphibole is from the vein shown in Figure 11 of Carlson and Zientek. Fluorian amphiboles have been noted in hydrothermal veins associated with granophyres at the Skaergaard intrusion (Bird et al., 1986), and F-rich alteration assemblages are found near granophyres in host rocks to the Skaergaard intrusion (Manning and Bird, 1990). Similar occurrence of F-bearing amphiboles in granophyric veins in the Stillwater Complex suggests that the fluid phase associated with granophyre formation in layered gabbros may commonly be enriched in F.

Pb-ISOTOPIC STUDIES

As part of an overall study of the Pb-isotopic systematics of the Stillwater Complex (Wooden et al., 1991),

TABLE 6. Electron-microprobe analyses and structural formulas for amphiboles in silicic veins

	87PPZ5				87PPZ3	
	Core	Rim	Core	Rim		
SiO ₂	57.4	55.9	56.4	55.2	52.4	51.3
Al ₂ O ₃	0.77	1.48	1.27	1.52	3.02	4.28
FeO ^T	3.07	6.07	5.08	8.54	10.1	11.5
MgO	22.7	20.6	21.2	18.9	17.6	16.6
CaO	13.9	13.6	13.9	13.5	13.0	12.8
Na ₂ O	0.09	0.16	0.14	0.15	0.43	0.58
K ₂ O	0.01	0.02	0.02	0.01	0.12	0.17
TiO ₂	0.05	0.08	0.08	0.05	0.18	0.20
MnO	0.02	0.08	0.05	0.07	0.11	0.08
Cl	0.02	0.02	0.02	0.02	0.04	0.04
F	0.07	0.03	0.06	0.01	0.19	0.21
Total*	98.10	98.04	98.22	97.97	97.19	97.76
Si	7.871	7.771	7.806	7.776	7.492	7.331
Al	0.125	0.229	0.194	0.224	0.508	0.669
Al	0.000	0.014	0.013	0.028	0.002	0.053
Fe ³⁺	0.000	0.077	0.000	0.055	0.257	0.356
Fe ²⁺	0.352	0.629	0.588	0.940	0.956	1.021
Mg	4.632	4.263	4.377	3.963	3.754	3.539
Ti	0.005	0.008	0.008	0.005	0.019	0.022
Mn	0.002	0.009	0.006	0.008	0.013	0.010
Ca	2.044	2.029	2.054	2.039	1.987	1.960
Na	0.000	0.000	0.000	0.000	0.013	0.040
Na	0.024	0.043	0.038	0.041	0.106	0.121
K	0.002	0.004	0.004	0.002	0.022	0.031

Note: Calculations based on 23 O atoms.
* Totals corrected for O = Cl + F.

Pb-isotopic data were obtained for whole-rock silicic samples and their feldspar separates (Table 7). Ages calculated from the whole rock and plagioclase (WR-PL) for the silicic rocks (Table 7) are younger than for the complex, suggesting varying reequilibration of the WR-PL Pb-isotopic systematics during a thermal event no earlier than about 2.1 Ga. Extreme Pb-isotopic ratios might have been anticipated from the varying and unusual Th-U ratios of the trace-element data. Backscattered-electron images show that equant zircon grains typically are zoned and heterogeneous (Fig. 6); they contain ill-defined micrometer-size areas of anomalous Th and U concentrations, minute (<1 μm) grains of uranothorite, and tiny (<2 μm) subhedral grains of galena (confirmed by electron microprobe).

With reservation, in view of these known complexities, we attempted to confirm the age of the silicic rocks as 2700 Ma. Uranium lead zircon data obtained for sample 86PPZ5 (Table 8) failed to confirm this age, however, yielding intercepts of 162 ± 45 Ma and 2132 ± 98 Ma on the concordia diagram; all points plotted rather linearly near the lower intercept, indicating a minimum of 74% Pb loss after about 2.1 Ga. Because of high U and Th contents, the zircons sustained heavy radiation damage, which would greatly facilitate Pb loss. Moreover, because of the large difference between the Pb-isotopic ratios for the whole rock and plagioclase separate, the WR-PL, common Pb age of 2580 Ma obtained for sample 86PPZ5 (Table 7) must be considered a reliable minimum age, indicating that the upper-concordia-intercept, uranium lead zircon age reflects an event significantly younger than the crystallization age. We interpret the U-Pb

TABLE 7. Pb-isotopic data for silicic rocks associated with the Stillwater Complex

Sample number	$^{206}\text{Pb}/^{204}\text{Pb}$	$^{207}\text{Pb}/^{204}\text{Pb}$	$^{206}\text{Pb}/^{204}\text{Pb}$	Pb (ppm)	WR-PL age (m.y.)
84CML16-PL*	184.580	49.184	64.440	0.67	2125
84CML16-WR	496.022	90.316	103.751	—	—
84PPC8-PL	21.299	16.671	34.543	—	2310
84PPC8-WR	46.793	20.416	39.098	5.52	—
84PPC2-PL	36.100	20.157	36.893	2.63	2310
84PPC2-WR	131.056	34.128	57.043	17.17	—
86PPZ5-PL	32.857	19.343	42.454	0.89	2580
86PPZ5-WR	334.554	71.381	175.040	—	—
S69-19-WR	508.570	123.370	132.270	0.79	—
Mouat quartz monzonite**	15.648	15.494	34.949	5.03	—
Average Stillwater cumulate†	13.95	14.95–15.01	33.6	0.33	2701 ± 8

Note: Analyst: Joseph L. Wooden.

* PL, plagioclase separate; WR, whole rock.

** Plagioclase from sample NB17-341.

† Apparent initial Pb-isotopic ratios for plagioclase separates, Wooden et al. (1991).

data to indicate a previously unknown influence in the Stillwater Complex of a 2.2–2.1 Ga thermal event. Apparently, because of heavy radiation damage, this event effectively reset the U-Pb isotopic systematics of the zircon, and measured data are not widely scattered, as might be expected for two-stage Pb loss. The zircon Pb-loss event at 2.2–2.1 Ga was apparently more effective in totally resetting the zircon ages than the WR-PL, common-Pb ages, which range from 2.6 to 2.1 Ga.

DISCUSSION

Extremely low K_2O contents and anomalously high CaO contents in rocks containing 77–79 wt% SiO_2 are difficult to explain by crystallization differentiation. This has been shown by Sinton and Byerly (1980), who described nearly holocrystalline dolerites from DSDP Hole 417D, which contain 0.5–1.5 vol% granophyric patches, that are compositionally similar to silicic rocks from midoceanic ridges. These irregular, interstitial patches, containing <0.3

wt% K_2O , are as much as 5 mm across and composed of fine-grained (<5 μm) irregular intergrowths of quartz and sodic plagioclase in subequal proportions. On the basis of textural relations, Sinton and Byerly concluded that the granophyric patches represent late-stage liquids, residual from at least 95–98% crystallization of the host dolerites, but that unusual processes are required to achieve such low K_2O contents. They noted that if K is treated as a completely incompatible element, 95% fractionation of a magma containing 0.08 wt% K_2O will produce a 5 wt% residual fraction containing 1.6 wt% K_2O . (Allowing for 40% fractionation of plagioclase containing 0.05 wt% K_2O still leaves 1.2 wt% K_2O in the residual melt.) Their line of reasoning poses greater problems in the case of the Stillwater granophyres because the parental magmas probably contained 0.25–0.29 wt% K_2O (Helz, 1985). Sinton and Byerly's proposal that a high-temperature vapor phase removed K during late-stage crystallization is not appealing to us as a solution to the problem because there is no theoretical or experimental evidence for such a process. In contrast, on the basis of pilot experiments, Jahns et al. (1969) suggested that granophyres in tholeiitic diabase may represent selective leaching of a quartz- and albite-rich fraction by an aqueous fluid, but their study was not pursued.

We propose that the silicic granophyres that transgress Banded-series cumulates of the Stillwater Complex represent accumulation of material through the action of an exsolved aqueous chloride solution (possibly augmented at times by equilibration of highly evolved residua with that solution) during or after the final stages of the cumulate-consolidation process. Similar but notably less specific conclusions were reached by Shannon (1924), by Walker (1940) in his study of the Palisades Sill, by Barker (1970) and Černý (1971) in the considering the development of granophyres and graphic granite in granitic rocks and pegmatites, and by Miyashiro et al. (1970) and Engel and Fisher (1975) for the most silicic oceanic plagiogranites. Pegmatitic segregations in medial parts of some veins and in the alaskite, deposition of Cr and chalcophile elements in selvages to the alaskite, anomalous Th/U ra-

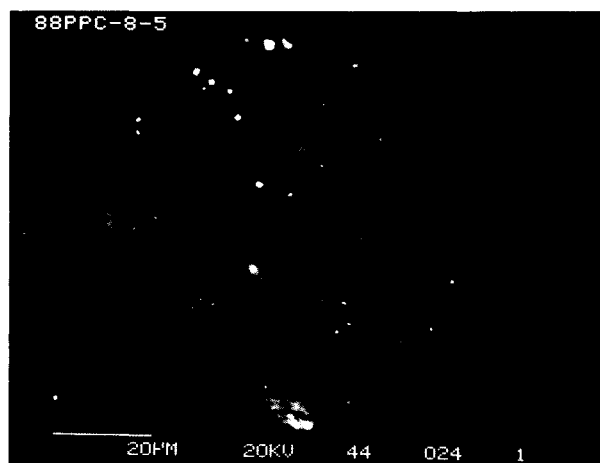


Fig. 6. Backscattered-electron image of zircon grain in plagioclase in sample 84PPC8. Bright squares, as much as 2 μm across, are galena inclusions; light gray areas within zircon are enriched in Th and U.

TABLE 8. U-Th data for zircons from sample 86PPZ5

Fraction	Description	U (ppm)	Th (ppm)	Th/U	Pb (ppm)
1	ten very clear grains; rare inclusions or discolorations	1444	249	0.172	35.874
2	13 oddball grains and fragments; some clear, some opaque	5110	926	0.181	667.23
4	12 euhedral grains; translucent to opaque, brown	6426	1255	0.195	657.92
5	13 large euhedral grains; translucent to opaque, brown	6845	873	0.128	628.81
6	19 large euhedral grains; translucent to opaque, brown	5684	969	0.171	605.15

Note: Analyst: Wayne R. Premo, U.S. Geological Survey.

tios, the presence of F-bearing amphibole, and rare hydrothermal leaching of adjacent cumulates are all consistent with precipitation from an aqueous solution.

A hydrothermal origin for the granophyres can be evaluated by examining the phase relations depicted in Figure 7. Figure 7A is a pressure-temperature projection showing selected equilibria involving plagioclase of composition An_{20} and the isobaric cooling path of the Stillwater intrusion. The polythermal, polybaric projection of H_2O -saturated plagioclase-melt equilibria are extrapolated from Johannes (1978, 1989). This diagram shows that the stability of An_{20} is defined at high temperatures by incongruent, H_2O -saturated melting and at low temperatures by reaction to zoisite, kyanite, quartz, H_2O , and plagioclase ($An_{<20}$). Taking the pressure of crystallization of the Stillwater Complex to have been 3.5 kbar (estimated at 3–4 kbar, Labotka, 1985) the diagram shows the An_{20} solidus to be at $\sim 720^\circ C$ in the presence of H_2O . Because plagioclase melts incongruently, An_{20} bulk compositions at supersolidus temperatures are represented by melts more sodic than An_{20} , in equilibrium with plagioclase more calcic than An_{20} . This increase in An content with increasing temperature is shown by the isopleths of constant composition in Figure 7A. Absence of zoning observed in the vein plagioclase strongly suggests that the granophyres do not represent the products of fractional crystallization of a magma. If they are magmatic, the granophyres must reflect a liquid emplaced on the An_{20} solidus.

The low-temperature stability of An_{20} is defined by reaction to a more sodic plagioclase, zoisite, kyanite, and quartz in the presence of H_2O (Fig. 7A; Goldsmith, 1982). This equilibrium was calculated by using the data of Berman (1988) for minerals, Haar et al. (1984) for H_2O , a standard-state convention of unit activity for stoichiometric minerals and H_2O at any pressure and temperature, and an activity of 0.32 for An_{20} (Schliestedt and Johannes, 1990). Figure 7A shows that An_{20} breakdown occurs below $300^\circ C$ at 3.5-kbar pressure. As noted above, late fractures filled by epidote are ubiquitous in the granophyres. If epidote of assumed composition of $Fe^{3+}/(Fe^{3+} + Al) = 0.33$ replaces zoisite in the breakdown reaction, and if clinozoisite activity in epidote is calculated with an ideal ionic mixing model, the minimum temperature of An_{20} stability is $340^\circ C$ at 3.5-kbar pressure.

These phase relations show that there is a wide range of temperature at 3.5-kbar pressure within which An_{20} is stable with quartz and H_2O . Figure 7B shows the solu-

bilities of SiO_2 , Na, and Al in H_2O at 3-kbar pressure. Molalities of SiO_2 correspond to equilibrium with quartz (Anderson and Burnham, 1965), and molalities of Na and Al correspond to equilibrium with albite (Davis, 1972, in Anderson and Burnham, 1983). Figure 7B shows that SiO_2 , Na, and Al solubilities increase with increasing temperature and that SiO_2 solubility is 0.7–0.9 log units higher than that of Na and Al at 500 – $700^\circ C$. Note that these solubilities are quite large; for example, at $700^\circ C$, SiO_2 concentration is 0.263 molal, which corresponds to 1.58 wt% SiO_2 in the fluid phase. Variations in chloride content will scarcely affect these solubilities (Anderson and Burnham, 1967, 1983; Orville, 1972). We attempted to use fluid-inclusion data from vein quartz to quantify directly the chemistry of the fluids associated with grano-

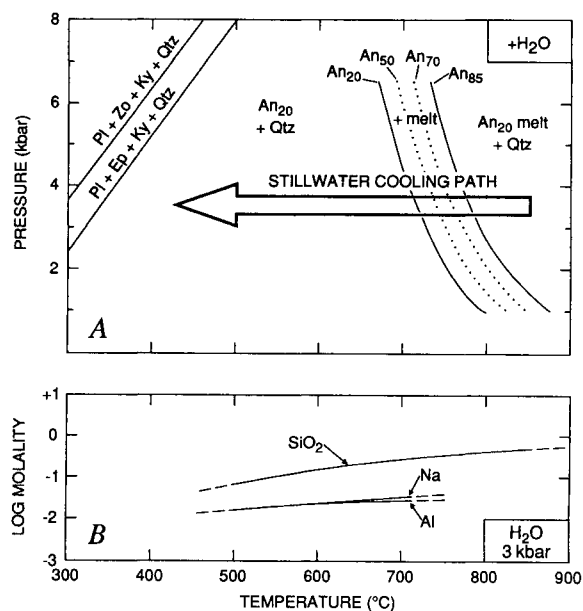


Fig. 7. (A) Pressure-temperature projection showing An_{20} phase relations in the presence of H_2O . Curves on right depict melting equilibria in the presence of quartz (Johannes, 1978, 1989); the An contents of plagioclase coexisting with the melt decrease from An_{85} on the liquidus to An_{20} on the solidus. Bold arrow portrays the assumed isobaric cooling path of the Stillwater Complex. (B) Solubilities of SiO_2 , Na, and Al in H_2O as a function of temperature at 3 kbar. Curve labeled SiO_2 is for equilibrium with quartz (Anderson and Burnham, 1965), whereas those labeled Na and Al are for equilibrium with albite (Davis, 1972).

phyre development, but we were foiled by an abundance of small, low-temperature secondary inclusions. Most of the identified inclusion types, however, contain tiny cubes of salt, probably halite.

Given the large solubilities of Na, Al, and SiO₂ indicated in Figure 7B, a sudden decrease in solubility clearly would lead to precipitation of quartz and albite. Such a decrease in solubility could be caused by isothermal opening of the fractures themselves. For example, if two reservoirs of fluid within the Stillwater Complex were at different pressures, a lower reservoir (the exsolved vapor phase) at lithostatic pressure, and an upper active hydrothermal reservoir (such as developed in the Upper Zone of the Skaergaard intrusion, Norton and Taylor, 1979) at sublithostatic pressure, and these reservoirs were separated by an impermeable thickness of cumulates, the sudden development of fractures generating hydraulic connectivity between the reservoirs would cause pressure to decrease in the high-pressure region. If this pressure drop were 500 bars, decreasing from 3.5 to 3 kbar, and the temperature remained constant at 500 °C, the solubilities of Na, Al, and SiO₂ in equilibrium with albite and quartz would decrease by 3.8, 3.2, and 27.5 mm, respectively, by least-squares fit to the data of Anderson and Burnham (1965, 1983) and Davis (1972). Assuming that a hypothetical 1-cm³ volume of granophyric vein material contains 60 vol% albite and 40% quartz, this 1-cm³ cube would contain 0.006 mol Na and Al and 0.036 mol SiO₂. On the basis of decrease in solubilities upon fracture opening, a maximum of 1.87 kg H₂O would be required to fill the 1-cm³ volume with albite and quartz. The 1-cm³ volume could be filled in 100 yr or less if fluid fluxes were greater than 5.9×10^{-7} g/s·cm². In their simulation of the cooling of the gabbroic Skaergaard intrusion, Norton and Taylor (1979) calculated somewhat lower fluxes as high as $\sim 2.5 \times 10^{-7}$ g/s·cm². However, their calculated fluxes are averages over 5.6×10^5 m³ of gabbro, and higher fluxes could be expected near concentrations of fractures. Our calculations suggest that the conditions required for rapid hydrothermal precipitation of the Stillwater granophyres are readily attainable at temperatures substantially below the An₂₀ solidus (Fig. 7A). Even lower fluxes would be required if temperatures were higher, if the pressure drop were larger, or if diffusive transport of aqueous species were considered in addition to advective transport.

The subsolidus cooling histories of gabbroic complexes probably varied widely, depending on factors such as the size of the complex, host rocks, depth of emplacement, and volatile content. Such factors significantly influence fluid flow and the degree of hydrothermal alteration. Nevertheless, there is good evidence that the Stillwater Complex hosted subsolidus migration of aqueous solutions (e.g., Boudreau et al., 1986; Boudreau and McCallum, 1986, 1989), and the calculations given above clearly show that, assuming reasonable fluxes, such fluids could have precipitated enough plagioclase and quartz to form the granophyres within short times.

Precipitation from an aqueous solution also explains the unusually low K and high Ca contents of the granophyres. Tie lines drawn by Orville (1963) for the Ca-free Ab-Or system indicate that a 2-*M* aqueous chloride solution at 2-kbar pressure and 600–700 °C will be in equilibrium with nearly pure albite if the molar ratio 100 K/(K + Na) in the fluid is less than 12. Moreover, Orville showed that the effects of chloride concentration and pressure are small, such that equilibria are little altered by total alkali chloride concentrations as low as 0.2 *M* or pressures as great as 5 kbar. The albitic granophyres of the Stillwater Complex could have been in equilibrium with an aqueous solution even richer in K, because Orville (1963) showed that the presence of Ca in the plagioclase increases the equilibrium K/(K + Na) ratio in the fluid.

Thus, the low K contents of the granophyres, nearly impossible to explain by crystallization differentiation, are predictable if they crystallized from an aqueous chloride solution. Furthermore, a solution-equilibrium model provides the best explanations for the Ca-rich composition of these veins containing 77 to 79 wt% SiO₂, for the occasional occurrence of K-rich perthite and amphibole in pegmatitic medial parts of veins, and for the late formation of throughgoing epidote veinlets. Crystallization differentiation probably could not produce rocks that contain 77–79 wt% SiO₂ and as much as 3.7 wt% CaO. However, Orville (1972, his Fig. 6) showed that at 700 °C and 2-kbar pressure, the Ca/(Ca + Na) ratio in plagioclase in equilibrium with an aqueous chloride solution will typically be relatively high. For example, fluid with a molar ratio of 100 Ca/(Ca + Na) \approx 3 is in equilibrium with plagioclase characterized by a 100 Ca/(Ca + Na) ratio near 18. (A granophyre composed of 60 vol% plagioclase of composition An₁₈ and 40 vol% quartz would contain about 2.3 wt% CaO.)

Our interpretation of the textural relation between K-free and K-bearing alkali feldspar shown in Figure 1B is that Na in the albite of early-formed albite-quartz granophyre was replaced by K from late-stage fluids that passed along the center of the vein. This rare occurrence of perthitic feldspar seems best explainable as a result of an increase in the molar proportions of K in the aqueous solution during the late stages of formation of some veins or, possibly, as a result of falling temperature as the granophyre-forming process waned. Orville (1963; see his Fig. 3) showed that as the fluid becomes richer in K, an albitic feldspar becomes richer in K; drastic shifts occur when the ratio 100 K/(K + Na) is in the range 23–28. At 700 °C (above the solvus in the alkali-feldspar system), alkali feldspar composition changes from Or₁₈Ab₈₂ to Or₅₈Ab₄₂ in response to a change from 25 to 28 mol% K in the fluid. At 600 °C, the solvus has been intersected, and a fluid containing 23.2 ± 0.5 mol% K is in equilibrium with two alkali feldspars. If fine perthitic texture can be taken as an indication that the feldspar was once homogeneous, formation of K-rich alkali feldspar must have taken place above 670 °C, solely because of the increasing

proportion of K in the fluid. However, if the texture can have another origin, falling temperature may have played a role in the K-enrichment process, because Orville showed that the fluid in equilibrium with two feldspars becomes progressively poorer in K as temperature falls. In fact, he cited hot-spring examples in which solutions containing only 3 mol% K, relative to total (K + Na), are replacing plagioclase with potassium feldspar. Regardless of origin, the compositions of the perthite components (Table 3) indicate that they have equilibrated at low temperature.

EPILOGUE

Although Orville's (1963, 1972) studies of cation exchange in aqueous chloride solutions have received the attention of aqueous geochemists and metamorphic petrologists, they appear to be poorly appreciated by igneous petrologists and students of pegmatite genesis. Summary articles on pegmatite genesis in Mineralogical Association of Canada Short Course Handbook Volume 8 and the R. H. Jahns Memorial Issue of *American Mineralogist* omit either report in their reference lists; only one or two papers in each volume cite Orville's papers.

Occurrence of granophyres in mafic cumulates of the Stillwater Complex has forced us to consider all options for the origin of these granophyres and ultimately to formulate a model for their origin that involves equilibria in aqueous solutions. Because pegmatites commonly occur in host rocks that contain potassium feldspar and a greater abundance of minor elements, it has been relatively easy and, certainly, popular to propose their origin as depending largely on crystallization from a magma. As we have indicated, however, processes involving cation-exchange equilibria afford ample opportunity to form feldspars with a broad range of textures and compositions that are extremely sensitive to evolving fluid compositions and changes in temperature. Černý (1971) interpreted graphic alkali feldspar + quartz and plagioclase + quartz intergrowths in some Czechoslovakian granitic pegmatites to be the last products of cotectic crystallization from an ultimately fractionated granitic magma. Associated, central blocky feldspar + quartz cores were assumed to have crystallized from supercritical gaseous fluids. Orville's studies show that regular progression along cotectic curves, used by Černý as a principal argument for crystallization fractionation, is also to be expected in a system evolving in equilibrium with an aqueous chloride solution.

We hope that this contribution will stimulate others to reexamine broadly the origin of late-stage siliceous rocks.

ACKNOWLEDGMENTS

We much appreciate the assistance of Carl Carlson in preparing the sketch map of the alaskite at Picket Pin Mountain. Robert F. Martin kindly characterized the albite typical of vein pegmatite, and numerous analysts provided grist for the mill. Perceptive reviews by Mary Donato, Bob and Reba Fournier, and Joe Wooden were useful, and discussions with Bob Fournier were especially helpful.

REFERENCES CITED

- Anderson, G.M., and Burnham, C.W. (1965) The solubility of quartz in supercritical water. *American Journal of Science*, 263, 494-511.
- (1967) Reactions of quartz and corundum with aqueous chloride and hydroxide solutions at high temperatures and pressures. *American Journal of Science*, 265, 12-27.
- (1983) Feldspar solubility and the transport of aluminum. *American Journal of Science*, 283-A, 283-297.
- Barker, D.S. (1970) Compositions of granophyre, myrmekite, and graphic granite. *Geological Society of America Bulletin*, 81, 3339-3350.
- Beeson, M.H., and Jackson, E.D. (1969) Chemical composition of altered chromites from the Stillwater Complex, Montana. *American Mineralogist*, 64, 1084-1100.
- Berman, R.G. (1988) Internally-consistent thermodynamic data for minerals in the system Na₂O-K₂O-CaO-MgO-FeO-Fe₂O₃-Al₂O₃-SiO₂-TiO₂-H₂O-CO₂. *Journal of Petrology*, 29, 445-522.
- Bird, D.K., Rogers, R.D., and Manning, C.E. (1986) Mineralized fracture systems of the Skaergaard intrusion. *Meddelelser om Grønland, Geoscience*, 16, 68 p.
- Boudreau, A.E., and McCallum, I.S. (1986) Investigations of the Stillwater Complex: II. The Picket Pin Pt/Pd deposit. *Economic Geology*, 81, 1953-1975.
- (1989) Investigations of the Stillwater Complex: Part V. Apatites as indicators of evolving fluid composition. *Contributions to Mineralogy and Petrology*, 102, 138-153.
- Boudreau, A.E., Mathez, E.A., and McCallum, I.S. (1986) Halogen geochemistry of the Stillwater and Bushveld Complexes: Evidence for transport of the platinum-group elements by Cl-rich fluids. *Journal of Petrology*, 27, 967-986.
- Bowen, N.L. (1915) Crystallization-differentiation in silicate liquids. *American Journal of Science*, 39, 161-185.
- Carlson, R.R., and Zientek, M.L. (1985) Guide to the Picket Pin Mountain area. In G.K. Czamanske and M.L. Zientek, Eds., *The Stillwater Complex, Montana: Geology and guide*, p. 262-276. Montana Bureau of Mines and Geology, Butte, Montana.
- Černý, P. (1971) Graphic intergrowths of feldspars and quartz in some Czechoslovak pegmatites. *Contributions to Mineralogy and Petrology*, 30, 343-355.
- Christiansen, E.H., Burt, D.M., Sheridan, M.F., and Wilson, R.T. (1983) The petrogenesis of topaz rhyolites from the western United States. *Contributions to Mineralogy and Petrology*, 83, 16-30.
- Coleman, R.G., and Donato, M.M. (1979) Oceanic plagiogranite revisited. In F. Barker, Ed., *Trondjemites, dacites, and related rocks*, p. 149-167. Elsevier, Amsterdam, The Netherlands.
- Coleman, R.G., and Peterman, Z.E. (1975) Oceanic plagiogranite. *Journal of Geophysical Research*, 80, 1099-1108.
- Conn, H.K. (1979) The Johns-Manville platinum-palladium prospect, Stillwater Complex, Montana, U.S.A. *Canadian Mineralogist*, 17, 463-468.
- Davis, N.F. (1972) Experimental studies in the system sodium-alumina trisilicate-water: Part I: The apparent solubility of albite in supercritical water, 322 p. Unpublished Ph.D. thesis, Pennsylvania State University, University Park, Pennsylvania.
- Engel, C.G., and Fisher, R.L. (1975) Granitic to ultramafic rock complexes of the Indian Ocean ridge system, western Indian Ocean. *Geological Society of America Bulletin*, 86, 1553-1578.
- Ernst, W.G. (1960) Diabase-granophyre relations in the Endion sill, Duluth, Minnesota. *Journal of Petrology*, 1, 286-303.
- Falconer, J.D. (1906) The igneous geology of the Bathgate and Linlithgow Hills. Part II. Petrography. *Royal Society of Edinburgh Transactions*, 45, 133-153.
- Gerlach, D.C., Leeman, W.P., and Avé Lallement, H.G. (1981) Petrology and geochemistry of plagiogranite in the Canyon Mountain ophiolite, Oregon. *Contributions to Mineralogy and Petrology*, 77, 82-92.
- Goldsmith, J.R. (1982) Plagioclase stability at elevated temperatures and pressures. *American Mineralogist*, 67, 653-675.
- Grout, F.F. (1918) A type of igneous differentiation. *Journal of Geology*, 26, 626-658.
- Haar, C., Gallagher, J.S., and Kell, G.S. (1984) NBS/NRS steam tables. Thermodynamic and transport properties and computer programs for

- vapor and liquid states of water in SI units, 400 p. Hemisphere, Washington, DC.
- Hamilton, W. (1959) Chemistry of granophyres from Wichita lopolith, Oklahoma. *Geological Society of America Bulletin*, 70, 1119–1126.
- Helz, R.T. (1985) Compositions of fine-grained mafic rocks from sills and dikes associated with the Stillwater Complex. In G.K. Czamanske and M.L. Zientek, Eds., *The Stillwater Complex, Montana: Geology and guide*, p. 97–117. Montana Bureau of Mines and Geology, Butte, Montana.
- Jahns, R.H., Martin, R.F., and Tuttle, O.F. (1969) Origin of granophyre in dikes and sills of tholeiitic diabase. *American Geophysical Union Transactions*, 50, 337.
- Johannes, W. (1978) Melting of plagioclase in the system Ab-An-H₂O and Qz-Ab-An-H₂O at $P_{H_2O} = 5$ kbars, an equilibrium problem. *Contributions to Mineralogy and Petrology*, 66, 295–303.
- (1989) Melting of plagioclase-quartz assemblages at 2 kb water pressure. *Contributions to Mineralogy and Petrology*, 103, 270–276.
- Labotka, T.C. (1985) Petrogenesis of the metamorphic rocks beneath the Stillwater Complex: Assemblages and conditions of metamorphism. In G.K. Czamanske and M.L. Zientek, Eds., *The Stillwater Complex, Montana: Geology and guide*, p. 70–76. Montana Bureau of Mines and Geology, Butte, Montana.
- Lambert, D.D., and Simmons, E.C. (1988) Magma evolution in the Stillwater Complex, Montana: II. Rare-earth element evidence for the formation of the J-M Reef. *Economic Geology*, 83, 1109–1126.
- Manning, C.E., and Bird, D.K. (1990) Fluorian garnets from the host rocks of the Skaergaard intrusion: Implications for metamorphic fluid composition. *American Mineralogist*, 75, 859–873.
- McDougall, I. (1962) Differentiation of the Tasmanian dolerites: Red Hill dolerite-granophyre association. *Geological Society of America Bulletin*, 73, 279–316.
- Miyashiro, A., Shido, F., and Ewing, M. (1970) Crystallization and differentiation in abyssal tholeiites and gabbros from mid-oceanic ridges. *Earth and Planetary Science Letters*, 7, 361–365.
- Norton, D., and Taylor, H.P., Jr. (1979) Quantitative simulation of the hydrothermal systems of crystallizing magmas on the basis of transport theory and oxygen isotope data: An analysis of the Skaergaard intrusion. *Journal of Petrology*, 20, 421–486.
- Orville, P.M. (1963) Alkali ion exchange between vapor and feldspar phases. *American Journal of Science*, 261, 201–237.
- (1972) Plagioclase cation exchange equilibria with aqueous chloride solution: Results at 700 °C and 2000 bars in the presence of quartz. *American Journal of Science*, 272, 234–272.
- Schliestedt, M., and Johannes, W. (1990) Cation exchange equilibria between plagioclase and aqueous chloride solution at 600 to 700 °C and 2 to 5 kb. *European Journal of Mineralogy*, 2, 283–295.
- Segerstrom, K., and Carlson, R.R. (1982) Geologic map of the banded upper zone of the Stillwater Complex and adjacent rocks, Stillwater, Sweet Grass, and Park Counties, Montana. U.S. Geological Survey Miscellaneous Investigations Series Map I-1383, 2 sheets, scale 1:24000.
- Shannon, E.V. (1924) The mineralogy and petrology of intrusive Triassic diabase at Goose Creek, Loudown County, Virginia. *U.S. National Museum Proceedings*, 66, 1–86.
- Sinton, J.M., and Byerly, G.R. (1980) Silicic differentiates of abyssal oceanic magmas: Evidence for late-magmatic vapor transport of potassium. *Earth and Planetary Science Letters*, 47, 423–430.
- Thompson, G. (1973) Trace-element distributions in fractionated oceanic rocks, 2. Gabbros and related rocks. *Chemical Geology*, 12, 99–111.
- von Eckermann, H. (1938) A contribution to the knowledge of the late sodic differentiates of basic eruptives. *Journal of Geology*, 46, 412–437.
- Walker, F. (1940) Differentiation of the Palisade diabase, New Jersey. *Geological Society of America Bulletin*, 51, 1059–1106.
- Wheatley, M.R., and Rock, N.M.S. (1988) SPIDER: A Macintosh program to generate normalized multi-element "spidergrams." *American Mineralogist*, 73, 919–921.
- Wooden, J.L., Czamanske, G.K., and Zientek, M.L. (1991) Lead isotopic study of the Stillwater Complex, Montana: Constraints on crustal contamination and source regions. *Contributions to Mineralogy and Petrology*, 107, 80–93.
- Zientek, M.L., Czamanske, G.K., and Irvine, T.N. (1985) Stratigraphy and nomenclature for the Stillwater Complex. In G.K. Czamanske and M.L. Zientek, Eds., *The Stillwater Complex, Montana: Geology and guide*, p. 21–32. Montana Bureau of Mines and Geology, Butte, Montana.

MANUSCRIPT RECEIVED JULY 12, 1990

MANUSCRIPT ACCEPTED MAY 20, 1991

APPENDIX 1. SAMPLE LOCATIONS AND DESCRIPTIONS

81CMC17. 45°28'01.2"N 110°08'15.6"W, fine-grained pbaC of the Gabbrozone II zone.

83BRL1. 45°30'49"N 110°13'45"W, magnetite-rich paC of the upper part of the Gabbrozone III zone (GN III)—the uppermost sample of Stillwater cumulates for which comparative chemical data are available.

84PPC8. 45°27'30"N 110°02'56.7"W, relatively unaltered pink vein, 10 cm thick, subparallel to cumulate layering of GN III. A crude bilateral symmetry is created by the occurrence of coarse-grained quartz and potassium feldspar along the central plane of the vein (Fig. 1B). Relatively coarse-grained granophyric intergrowths (albitic component as large as 3 × 5 to 2 × 7 mm) along vein margins give way to finer grained, granophyric to graphic-textured "flames," 1–2 cm wide and approximately 3 cm long, that apparently grew toward the vein center (Figs. 1B and 2B).

84CML16. 45°28'13"N 110°08'41.7"W, vein, 5 cm wide, cutting uppermost cumulates (poC) of Olivine-bearing zone II. Continuous epidote veinlet, 1–2 mm thick, lies approximately 1 cm from one vein margin. Entire white to pale-pink vein is characterized by classic granophyric textures (Figs. 1A and 2A).

85PPC2. 45°27'30"N 110°02'56.7"W, relatively unaltered pink vein, 2.5–3 cm wide, cutting cumulates of GN III. Albitic portions of granophyric intergrowths near the vein margin may be as large as 2 × 4 mm, whereas significantly finer grained intergrowths approaching graphic texture are found near the center of the vein.

86PPZ5. 45°26'17"N 110°03'02"W, alaskite with quartz and altered plagioclase grains, each 1–3 mm across; quartz grains commonly form branching aggregates several centimeters long. Contacts between quartz aggregates and plagioclase commonly are highly irregular because of incipient development of graphic textures between the two minerals, such that large quartz grains commonly are bordered by optically continuous, fine-grained satellites. Small (0.1 × 1 mm) grains of chlorite (after biotite?) constitute approximately 1 vol% of the rock, and titanite (to 0.3 mm) is a notable minor phase. Minor epidote is present.

87MVZ2. 45°23'24"N 109°54'30"W, relatively fresh vein, 5 cm wide, cutting the Norite I zone. Texture is dominantly allotriomorphic granular (average grain size, 3 mm), with only sparse development of patchy quartz grains suggestive of granophyric texture. A discontinuous subparallel veinlet (max 5 mm wide) of similar texture is 2.5 cm away. Along the far margin of the veinlet, as well as 1.5 cm from the main vein, are veinlets of epidote, 0.5–2 mm wide.

87PPZ1. 45°27'22"N 110°02'52"W, light-pink vein, 7.5–9 cm thick, semiconcordant to well-laminated cumulates of GN III. One side of the vein is a 2.5–3-cm thickness of flame granophyre comparable to that of sample 84PPC8; granophyre is more irregular in thickness on the opposite side of the vein. The rest of the vein is an irregular but sharply bounded core of coarse-grained (maximum 1.5 × 4 cm) pegmatite, composed of quartz and near

end-member albite. Separated from the granophyric margin of the vein by 0.8–2.5 cm of cumulate is an irregular veinlet of granophyre that tapers from 11 to 1 mm over 20 mm and encloses several long, undisturbed pyroxene needles from the host cumulate.

87PPZ3. 45°27'22.2"N 110°02'52.2"W (Carlson and Zientek, 1985, Fig. 1, locality 13), compound vein, 8 cm wide, including 1-cm-thick septum of cumulate parallel to one wall of vein. Irregular veinlet of coarse-grained epidote, 1.5–7 mm thick, lies within the vein 0.5–1.5 mm from the other contact with medium-grained gabbro-norite (pbaC) of GN III. Clots of actinolitic amphibole grains (maximum 1 × 10 mm) lie in medial areas of vein. Bulk of the vein is medium-grained feldspar-quartz intergrowth.

87PPZ5. 45°27'58.1"N 110°02'51.1"W (Carlson and Zientek, 1985, Fig. 1, locality 18), vein, 8–9 cm wide, containing actinolitic amphibole (maximum 1 × 10 mm) in clots as much as 4 cm across. Continuous veinlet, 1.5–2 mm wide, of coarse-grained epidote intergrown with quartz lies 0.5–2 mm from one contact with fine-grained gabbro-norite (pbaC) of GN III. Alteration of pyroxene in the gabbro-norite decreases away from the vein. At the vein walls adjacent to cumulates is a near-monomineralic zone (1–2 cm wide) of altered (pale pink), coarse-grained plagioclase. Intermediate parts of the vein may display classic granophyric textures (widths of feldspar and quartz components, 0.3–1.5 mm). Much of the core of the vein is a pegmatoidal intergrowth of quartz and feldspar, with quartz predominant.

87PPZ6. 45°26'16"N 110°02'59"W, contact between alaskite of Picket Pin Mountain and plagioclase cumulates of the Anorthosite I zone. Irregular, dark, chromite-rich selvage (approx-

mately 5 cm thick) separates the two rock types. The plagioclase cumulates are extensively altered to epidote and chlorite, such that grain shapes and texture are unrecognizable. The alaskite is also altered, with extensive texture-disrupting formation of epidote (blades maximum 12 mm long near selvage). Sparse large, subhedral, zoned allanite grains in alaskite can measure 6 × 14 mm.

87PPZ29. 45°27'14.4"N 110°02'43.3"W, vein 2.5 cm thick, and veinlet, 4 mm thick, separated by a fragment of cumulate 1 cm thick. The vein consists primarily of coarse-grained granophyre but has an irregular, quartz-rich central zone containing an altered mafic phase. Pyroxene in host cumulate of GN III is extensively altered to amphibole.

87TAZ5. 45°28'22"N 110°04'58"W, aplitic-textured vein, 7 cm thick, nearly conformable with heavily altered cumulates of Olivine-bearing zone V. Plagioclase phenocrysts may be 1 mm long, but average grain size is 0.2–0.6 mm, with many subrounded grains <0.1 mm across.

NB17-341. 45°22'02"N 109°49'24"W, typical sample (from drill core) of the Mouat quartz monzonite, a pluton (believed partly to represent crustal melting) that intruded the Stillwater Complex shortly after its emplacement.

S69-19. 45°26'16.2"N 110°02'58"W, alaskite in which aggregates of quartz (maximum 4 × 5 mm) and altered plagioclase grains (maximum 3 × 5 mm) are intricately intergrown. Quartz has very uneven extinction, with domains commonly <0.1 mm across. Moreover, quartz aggregates are typically surrounded by haloes of highly irregular, subrounded, tiny quartz grains. The texture may be related to the more angular, subgraphic texture found in sample 86PPZ5.